Spectroscopic Studies of Human Hair, Nail, and Saliva Samples Using a Cantilever-Based Photoacoustic Detection

Jaakko Lehtinen

International Journal of Thermophysics
Journal of Thermophysical Properties and Thermophysics and Its Applications

ISSN 0195-928X

Int J Thermophys
DOI 10.1007/s10765-013-1488-x

Springer

Int J Thermophys
DOI 10.1007/s10765-013-1488-x

Spectroscopic Studies of Human Hair, Nail, and Saliva Samples Using a Cantilever-Based Photoacoustic Detection

Jaakko Lehtinen

Received: 27 January 2012 / Accepted: 12 July 2012

Abstract In infrared spectroscopy human hair has normally been studied using attenuated total reflectance or diffuse reflectance infrared Fourier transform spectroscopy, for which the sample preparation methods can lead to problems of reproducibility. Definite information could be obtained by studying intact individual hair fibers, but the small diameter of hair fibers and the lack of sensitivity make such measurement difficult. A highly detailed infrared spectrum of human hair has been measured using a cantilever-based photoacoustic detection. The spectrum can be obtained even if a piece of hair as small as 1 cm is used as a sample. Photoacoustic spectroscopy (PAS) is a well-established technique in many areas, but very little has been published in the research of proteins. Two simple applications of PAS for human hair, as well as measurements with different types of proteins, are presented in this paper.

Keywords Cantilever · Depth profiling · Hair · Keratin · Photoacoustic spectroscopy

1 Introduction

Fourier transform infrared–photoacoustic spectroscopy (FTIR–PAS) is an infrared sampling technique widely used in research and industry. Its main advantage is to be able to measure FTIR spectra on basically any sample without the common sample preparation techniques used in infrared spectroscopy [1]. In many cases, direct measurements with conventional transmission—or reflection—based infrared techniques are inappropriate, or have limitations [2]. Photoacoustic detection does not require the sample to be transmitting, has little sensitivity to the morphology of the

J. Lehtinen (✉)
Laboratory of Optics and Spectroscopy, Department of Physics and Astronomy, University of Turku, Vesilinnantie 5, 20014 Turku, Finland
e-mail: jaaleht@utu.fi

Published online: 28 July 2013

sample surface, and enables different sampling depths to probe inhomogenous samples [1,2]. The photoacoustic signal is proportional to the optical absorption coefficient. Instead of measuring transmitted or reflected photons, the acoustic signal, generated by the heating of sample due to absorption of photons, is examined [3]. Photoacoustic infrared spectroscopy is a valuable tool for studying solid samples of various morphologies due to the ease of sample preparation and depth profiling capabilities. PAS is an ideal technique for most of the commonly difficult samples in infrared spectroscopy.

Human hair, as well as nails and skin, consists of fibrous structural proteins that are generally called keratin, and carry a lot of information on an individual within its composition [4]. Hair has been proved to monitor diseases [5], drugs of abuse [6,7], chemical treatments and weathering [8], or even malnutrition [4]. All of the above features can be discovered using infrared spectroscopy. Most of the information is also nearly permanent in hair [5,6]. In addition to the applications in infrared spectroscopy of hair, saliva has been used for the detection of diabetes, and fingernails have been used for an index of health and diseases [9,10]. In infrared spectroscopy, attenuated total reflectance (ATR) or diffuse reflectance infrared Fourier transform spectroscopy (DRIFTS) has mainly been used to study human hair. In addition, Raman spectroscopy has been used as a complementary technique. In the above-mentioned techniques a microtome, or similar mechanical device operating at micrometer precision, is normally needed in hair sample preparation procedures. After cutting to the desired length and form, the hair is usually mounted in paraffin wax or similar to enable the measurement. With photoacoustic detection, the sample preparation can be done with only scissors and a pair of fine tweezers. The irregular shape of hair fiber creates no problem since the photoacoustic method is not affected by scattering or reflecting [3]. PAS is one of the few infrared techniques that enable depth profiling performed from the sample surface. Other techniques that provide depth-sensitive information include ATR, DRIFTS, and Raman spectroscopy with a confocal microscope [11–13]. Photoacoustic signal can also be obtained from completely black samples, which is a common problem with most infrared techniques.

In this study, an interferometric cantilever microphone was used as a pressure sensor. Condenser microphones that are commonly used in photoacoustic systems work at their physical limits, and therefore there is no way to further improve their sensitivity. The interferometric cantilever microphone can be constructed in such a manner that the sensitivity is even several orders of magnitude higher than the one of the condenser microphone [14,15]. A typical cantilever microphone consists of a 5 μm to 10 μm thick silicon cantilever and a Michelson interferometer to measure the position of the cantilever. When the pressure in the cantilever cell varies, the cantilever bends but it does not stretch. Therefore, it is very sensitive to pressure variations compared to the stretching of the elastic membrane of the condenser microphone [14]. The cantilever dynamics and noise sources are carefully modeled in the literature and thus the performance of the cantilever microphone is well known. The lack of sensitivity has previously been a limiting factor for the use of the photoacoustic method in FTIR applications. Using acoustical resonances of the sample cell is a common way to enhance the sensitivity, but the wide frequency band needed by the FTIR instruments makes such devices not useful in the FTIR applications. The cantilever microphone,

however, has a wide frequency band and a sensitivity even several orders higher than the conventional microphones [14].

In this paper, the mid-infrared photoacoustic spectrum of hair has been successfully measured using a cantilever microphone and the basic features of the spectra have been explained. Adequate signal levels could even be obtained from a single hair fiber with a length of less than 1 cm. All of the characteristic features can also be identified in the spectrum of a single fiber. In this study, however, more hair fibers were used to ensure a reliable signal-to-noise ratio (SNR) in precise examination. In addition, spectra of nail and saliva samples have been measured for comparison. Nails are similar keratin to hair, and saliva contains a complex mixture of proteins. The main issue of this paper is to demonstrate briefly two important applications with this new method of investigation. These include a method to study chemical treatments, and a simple approach to depth profiling.

2 Experimental

All the samples were measured using a Gasera PA301 cantilever enhanced photoacoustic detector coupled with a Thermo Nicolet, or a Bruker Tensor FTIR spectrometer. The photoacoustic detector was used as an external detector for the FTIR instrument. PA301 consists of the actual detector and a DSP module, which contains mathematics for the optical cantilever microphone. The minimum detectable pressure variation in the PA301 sample cell is $2\,\mu\mathrm{Pa}\cdot(\sqrt{\mathrm{Hz}})^{-1}$ and the microphone sensitivity is approximately $10\,\mathrm{V}\cdot\mathrm{Pa}^{-1}$. Usable spectrometer scan velocities can be 5 Hz to 30 kHz with this detector, but this is limited by the spectrometers used in this study to 2.2 kHz to 20 kHz. The FTIR spectrometers used were standard laboratory instruments working in the mid-infrared area. In this study, the usable wavenumber region was approximately $\nu = 800\,\mathrm{cm}^{-1}$ to $4000\,\mathrm{cm}^{-1}$. The superior sensitivity of the cantilever-based detector, compared to other commercial products, is directly reflected in the measurement times, as the SNR is proportional to the square root of measurement time. The cantilever microphone is proved to be approximately 100 times more sensitive than a capacitive microphone in trace-gas sensing [16], which means 10 000-fold measurement times with the capacitive microphone to acquire the same SNR. The case is usually not as good with solids, but generally ten times better sensitivity is reached.

Hair samples were collected from the tip of the hair from a male and a female person in their mid-twenties. Fingernail and saliva samples were collected only from the male. Hair fibers were cut into approximately 2 mm pieces, and laid on the bottom of the sample cup. A composition of individual hair fibers was used to obtain a good average. The sample preparation was done with a pair of tweezers and scissors. The sample cup had a cylindrical form with a 10 mm diameter, and a height of 2 mm, and it was filled almost completely with hair fiber material. Also, single hair fibers approximately 1 cm in length were studied. The sample cups were cleansed with an ultrasonic cleaning device to minimize the effects of possible traces in the cups. The sample preparation methods for fingernails were similar to hair. Saliva samples were collected straight into the sample cup, and left to dry in room temperature for about 16 h. Dry saliva samples were used in the measurements to minimize the collaboration of water in the spectrum. Liquid saliva samples could also be measured with the setup used in

this study. Typically a 24 h fasting is required when collecting saliva samples and the samples are usually frozen for reliable storage. Fasting is required since saliva depends on daily diet and freezing prevents the proteins from degradation and denaturation [17]. In this study, however, a simple approach was used for a quick comparison, and the main focus was kept on the analysis of hair. The photoacoustic cell and the sample cell were purged with helium before the measurements for enhanced signal. The spectra were normalized using a carbon black reference. An 8 cm^{-1} resolution, 20 scans for approximately 40 s measurement time, and a 2.2 kHz (Bruker) or 2.5 kHz (Thermo) scan velocity were the parameters used in measurements. 100 scans were used with single hair fibers for a greater SNR. A solution with one-fifth hydrogen peroxide (30 % solution), one-fifth ammonium hydroxide (25 % solution), and three-fifths water was used to bleach the hair samples in the treatment studies. The hair fibers were immersed in the mixture for 1 h, then rinsed under running water, and finally left to dry. A sufficiently long bleaching time was used to illustrate the differences between a normal coloring effect and a much harsher treatment.

3 Results and Discussion

In Sect. 1, it was mentioned that hair consists mostly of fibrous proteins that are generally called keratin. Keratins are long chains of amino acids linked together with amide bonds. In addition to keratin, hair contains water, lipids, and trace elements. Therefore, the infrared spectrum of human hair retains features of different vibrational modes of the amide bond, different individual amino acids, lipids and fatty acids, bonded water, and trace elements. Amino acids and amide bonds are the basic elements to be investigated in this study. The diameter of hair fibers varies from 30 μm to 120 μm. Hair fiber consists of three different layers which are called cuticle, cortex, and medulla, from the surface to the center. The cuticle is a 5 μm to 10 μm thick chemically resistant layer consisting of flat overlapping cells [4]. The cuticle is wrapped around the cortex, which contributes to the major part of the mass in human hair. The 40 μm to 60 μm thick cortex consists of elongated cells and intercellular binding material [4,18]. Inside the cortex, a third type of cell, the medulla, may be found. Medulla can be absent, continuous, or discontinuous along the fiber axis in human hair [4]. The cuticle and cortex are the layers that can be reached with this setup. The minimum scan velocity of the spectrometers used in this study corresponds to a thermal diffusion length too short to reach the medulla. Step-scan spectrometers, or infrared sources with wider sweep of modulation frequencies, can overcome this problem. Fingernails are composed of three different layers of keratin laying on the top of the nail bed [19]. The outermost part consists of the narrow dorsal layer, which gives rise to the laminated nail surface [20]. Below the dorsal layer is a thicker and harder layer, called the intermediate layer, and on the bottom lies the narrow ventral layer [19]. Saliva is a complex mixture of proteins and other molecules originating from different sources. Saliva is formed primarily from salivary gland secretions, but it can also have contribution for example from blood, oral tissues, and food remainings. Saliva consists mostly of water, proteins, and inorganic and trace substances. Human saliva contains more than 1000 peptides or proteins that have important biological functions [17]. Unlike the proteins in hair and nail, salivary proteins are different from keratin.

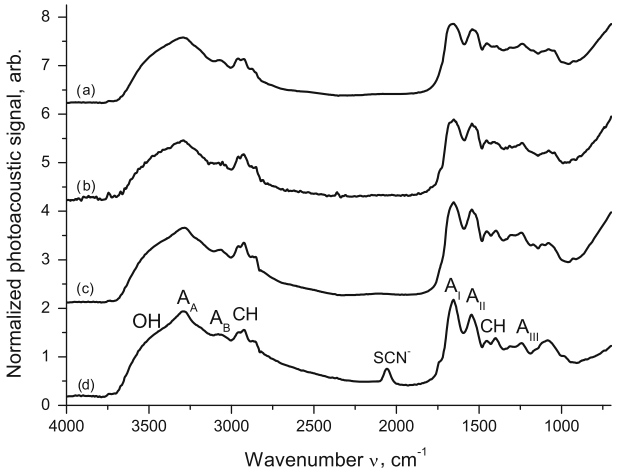

Fig. 1 Different types of keratin, and saliva proteins measured with FTIR–PAS. Photoacoustic signal was normalized with carbon black sample and is shown in arbitrary units: (a) hair sample (composition), (b) hair sample (single fiber), (c) fingernail sample, and (d) saliva sample. Notations A_A, A_B, A_I, A_{II}, and A_{III} in the figure represent amide A, B, I, II, and III peaks, respectively. CH represents CH_2 and CH_3 peaks of lipids and fatty acids and OH signifies bonded water in spectra. Thermo FTIR was used in these measurements

3.1 Measurements with Different Types of Proteins

In Fig. 1, we can see the measured spectra of two different hair samples, a nail sample, and a saliva sample from the same person. The first hair sample was a composition of hair fibers prepared in the manner introduced in Sect. 2, and the latter was a single 1 cm piece of hair. In this figure we can see that the four spectra look quite similar, and have the same characteristic features and spectral peaks. We can also conclude that the spectra of two different hair samples are almost completely similar, only with different SNRs. Amide A, B, I, II, and III peaks (labeled A_A, A_B, A_I, A_{II}, and A_{III} in Fig. 1) dominate the spectra around $\nu = 3300\,\mathrm{cm}^{-1}$, $\nu = 3070\,\mathrm{cm}^{-1}$, $\nu = 1655\,\mathrm{cm}^{-1}$, $\nu = 1545\,\mathrm{cm}^{-1}$, and $\nu = 1245\,\mathrm{cm}^{-1}$, respectively, followed by lipids and fatty acids (CH) at $\nu = 1350\,\mathrm{cm}^{-1}$ to $1480\,\mathrm{cm}^{-1}$ and $\nu = 2900\,\mathrm{cm}^{-1}$ to $3000\,\mathrm{cm}^{-1}$, and bonded water (OH) around $\nu = 3500\,\mathrm{cm}^{-1}$. The only radical difference between the spectra is the $\nu = 2058\,\mathrm{cm}^{-1}$ peak in the spectrum of saliva, which belongs to the antibacterial compound thiocyanate (SCN^-) [21]. Besides that, the differences relate to the shapes and ratios of certain peaks, rather than finding characteristic peaks for the different sample materials. When comparing amide I and II peaks we can see that the peak shape varies notably between different samples. This is related to the different secondary structure of proteins, i.e., the different formations of amino acid chains [20]. In Table 1, we can see the ratio of the amide I and II peak intensities, full width at half-height (FWHH) of amide I peak, and positions for the amide I and II peak maxima calculated for each sample material to further illustrate the differences in amide I and II areas. FWHH is calculated using the minimum between the amide I and II peaks as a minimum of the amide I peak. In Table 1, we can see that the amide I peak of the saliva sample is the narrowest, and has the highest intensity compared to the amide II peak.

Table 1 Different parameters calculated from the measurement data to demonstrate the variation in the amide I and II bands between different sample materials

Sample	A_I/A_{II} ratio	A_I FWHH (cm^{-1})	A_I position (cm^{-1})	A_{II} position (cm^{-1})
Hair (Fig. 1a)	1.07	78.6	1654	1540
Fingernail	1.07	67.5	1653	1543
Saliva	1.16	57.4	1655	1545

Hair has the broadest amide peaks of the measured samples. We can also see slight differences in positions of the amide I and II peak maxima between different samples in Table 1. Other notable differences in the spectra are in the stretching and bending modes of CH_2 and CH_3 of lipids and methyl groups in $\nu = 1350\,cm^{-1}$ to $1480\,cm^{-1}$, and $\nu = 2900\,cm^{-1}$ to $3000\,cm^{-1}$. Also, the $\nu = 1000\,cm^{-1}$ to $1150\,cm^{-1}$ area of saliva sample differs from the others. Since the spectra of different proteins are essentially similar, it is possible to also expand the results and knowledge of hair to other keratin and protein sources. In addition, other types of keratin can be used in conjunction with hair for broader investigation of hair keratin, as in this study.

3.2 Bleaching Studies

Some everyday processes like washing hair, combing, and exposure to sunlight affect the composition of hair [4]. Similar, but stronger, effects can be seen in colored, bleached, or permanented hair. Levels of the amino acids cystine and cysteine have been studied carefully in the literature with multiple different methods. This is because cystine and cysteine appear in high concentrations in hair, and they are also highly reactive. Chemical treatments and weathering are easily studied by comparing cystine and cysteine levels with their derivatives. The chemical reaction that can be observed in these processes is the fission of C–S bond into sulfonate S=O bond by oxidation [4].

In Fig. 2, we can see the effects of chemical treatment in the photoacoustic infrared spectrum of hair. Figure 2 shows spectra for non-treated male, colored female, and bleached male hair samples. The spectra were baseline corrected between $\nu = 1000\,cm^{-1}$ to $1700\,cm^{-1}$ and normalized to the amide II peak after baseline correction. The baseline was corrected to standardize the spectra and ease the comparison between different samples as the baseline varies slightly in every sample. The differences in baseline arise from the slight variations in sample cell volume, and sample position, due to different sample sizes [22,23]. This effect has to be taken into consideration since the sample fills the sample cup irregularly, and therefore the cell size and the average sample height vary with every sample. The spectrum of non-treated hair was also subtracted from spectra of colored and treated hair samples to obtain difference spectra. This was to emphasize the differences between treated and non-treated samples, and to obtain a more straightforward comparison in Fig. 2.

The most notable feature in the spectra of treated hair samples is the rise of intensity of the peak at $\nu = 1042\,cm^{-1}$ that relates to the symmetric S=O stretching band of sulfonates [24–26]. In addition, a smoother slope between $\nu = 1120\,cm^{-1}$ and $\nu = 1260\,cm^{-1}$ can be discerned. This observation relates to the overlapping peaks of asymmetric S=O stretching band of sulfonates at $\nu = 1188\,cm^{-1}$, asymmetric S=O stretching of thiosulfate ions at $\nu = 1196\,cm^{-1}$ [24], and cysteic acid moiety

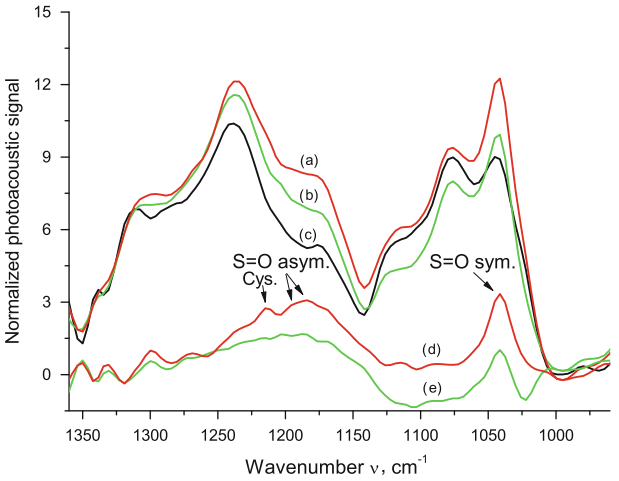

Fig. 2 The effect of coloring and hydrogen peroxide treatment: (a) bleached hair sample, (b) colored hair sample, (c) non-treated hair sample, (d) difference spectrum of bleached and non-treated hair samples, and (e) difference spectrum of colored and non-treated hair samples. Positions of asymmetric and symmetric S=O stretching as well as cysteic acid moiety are marked in the figure. Bruker FTIR was used in these measurements

(Cys. in Fig. 2) at $\nu = 1219\,\mathrm{cm}^{-1}$ [24,25]. The cysteic acid moiety peak can be easily distinguished only in the difference spectrum of bleached hair due to the harsh treatment. The effects of coloring and bleaching could be marked out in the spectra, but the intensity of the treatment can also be investigated. This can be done by studying the ratio of $\nu = 1042\,\mathrm{cm}^{-1}$ and $\nu = 1076\,\mathrm{cm}^{-1}$ peaks. If hair is exposed to treatments or weathering, the intensity of the S=O peak at $\nu = 1042\,\mathrm{cm}^{-1}$ rises, and this effect can be quantified by calculating the $\nu = 1042\,\mathrm{cm}^{-1}$ and $\nu = 1076\,\mathrm{cm}^{-1}$ peak ratio. In Fig. 2, we can see how the ratio rises with the intensity of the treatment.

3.3 Depth Profiling Studies

A rough simplification of depth profiling was made to demonstrate this advantageous feature of photoacoustic spectroscopy with hair samples. The spectrum of the same hair sample was measured with two clearly different FTIR scan velocities to obtain two different sampling depths. With fast scan velocities the thermal diffusion length is short, and we obtain information only from layers at the surface. With lower scan velocities the thermal diffusion waves can propagate a longer distance, and we get information also from the layers that lie deeper in the sample. The spectra were recorded with 2.2 kHz and 10 kHz scan velocities that correspond approximately to a 3.2 μm to 9.2 μm and 1.6 μm to 4.6 μm thermal diffusion lengths in the $\nu = 500\,\mathrm{cm}^{-1}$ to $4000\,\mathrm{cm}^{-1}$ wavenumber range [27]. A zero filling factor of 8 was used to obtain data points at intervals of $1\,\mathrm{cm}^{-1}$ for better defined peaks in the spectrum. The saturation compensation method, demonstrated by McClelland et al. [1], was used to enable practical comparison of spectra measured with different sampling depths. Saturation

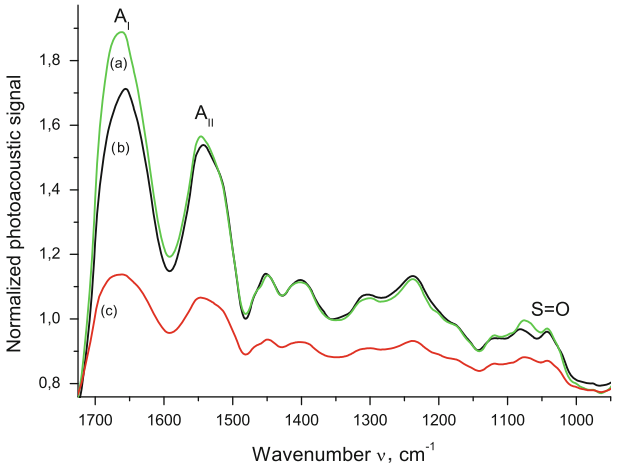

Fig. 3 A simple approach to depth profiling. Spectrum of a same hair sample is shown with three different configurations: (a) 2.2 kHz spectrum with saturation compensation, (b) 10 kHz spectrum, and (c) 2.2 kHz without saturation compensation. Bruker FTIR was used in these measurements

compensation is generally used to remove the saturation differences while retaining any differences related to sample structure. When the scan velocity is increased, the bands that are saturated increase relative to weaker bands, due to reduction of saturation effects [1]. The use of linearization or a saturation compensation algorithm is particularly important in this case, where the photoacoustic signal is mostly non-zero. This means that some level of saturation can be found all over the spectrum. This simple saturation compensation algorithm applies only to a magnitude spectrum, whereas linearization methods use both phase and magnitude spectra. In Fig. 3, we can see a spectrum measured with 10 kHz scan velocity, and spectra for 2.2 kHz scan velocity before and after saturation compensation. In this figure we can instantly see that spectra of hair samples with radically different mirror velocities are basically incomparable before the saturation compensation.

If we compare the compensated spectra with different scan velocities, we first see the great differences in the amide I peak at $\nu = 1655\,\mathrm{cm}^{-1}$. The amide I peak can often be out of the linear range of Beer's law [25], and is therefore too saturated for the compensation algorithm. Saturation can also be a problem with the amide II peak, as it has the second highest intensity. Jurdana et al. [27] found the saturation of a photoacoustic signal a problem with hair samples as well, especially in the amide I and II peak areas. Based on our own experience, and the results of previous studies [25,27], we do not use the heights of amide I and II peaks as a reliable measure in our comparison, although the saturation compensation algorithm seems to maintain the intensity of the amide II peak quite well in our case. The differences in heights of the amide I, and also the amide II, are believed to occur mainly from the effects of saturation. Additionally, we found differences in the positions of the amide I and II peaks, which are an actual feature. The amide I and II peaks shift to lower wavenumbers as the scan velocity is increased.

Protein secondary structures and multiple individual amino acids are infrared active in amide I and II regions [20,28]. Differences in spectra are related to the different

protein secondary structures, and different amino acid compositions between the surface layer cuticle and inner layer cortex. With a 10 kHz mirror velocity, the signal comes only from the 5 μm thick cuticle [4], and with a 2.2 kHz mirror velocity, from both cuticle and cortex. This shifting of amide I and II peaks in different layers of hair has also been noted by other groups with different infrared techniques [24,27]. Another clear feature that could be marked out was the differences at the S=O stretching area between $\nu = 1040\,\mathrm{cm}^{-1}$ to $1260\,\mathrm{cm}^{-1}$. The ratio of $\nu = 1042\,\mathrm{cm}^{-1}$ and $\nu = 1076\,\mathrm{cm}^{-1}$ peaks is the quantity to be investigated, as stated previously in Sect. 3.2. The ratio of the peaks is higher in the 10 kHz spectrum, which indicates that the layers near the surface are more weathered than the layers deeper in hair.

The differences founded are logical since the cuticle is more strongly exposed to the sunlight, chemical treatments, and mechanical stress than the cortex. The depth profiling measurements were performed rapidly, as nothing had to be done to the sample to achieve different sampling depths. The only thing to be altered was the parameters of the FTIR instrument. Photoacoustic depth profiling thus offers a valuable and easy tool for investigation of heterogeneous tissues like hair.

4 Conclusions

We examined human hair with cantilever-based photoacoustic detection. Highly detailed spectra can be obtained from a small amount of hair keratin with short measuring and sample preparation times. Simple depth profiling and chemical treatment experiments were presented as successfully demonstrating the possible applications to human hair with this technique. Similar spectra can also be obtained from other sources of keratin or proteins. A composition of short hair fibers was used as a sample to maximize the SNR for precise examination. Cantilever PAS also showed promising results with single hair studies in which the sample can be less than 1 cm of hair fiber. Single hair studies have typically suffered from low reproducibility and lack of sensitivity.

PAS is a simple and effective method for rapid measurements with condensed matter. Photoacoustic detection yields great advantages in sample preparation methods when compared to other common infrared techniques. This is particularly important in study of human hair and other fibrous materials, which usually require complicated sample preparation methods. Sample preparation advantages, combined with the extreme sensitivity of the photoacoustic technique and cantilever microphone, make this method significantly faster and easier than other similar approaches. In addition, PAS is one of the few infrared techniques with the possibility to perform depth profiling from the sample surface.

Hair appears to be the most promising sample type in means of sample preparation and time span. Saliva requires more difficult sample preparation and storage methods, and is also highly affected by recent food history. Fingernails are usually cut more often than hair, and therefore carry information from a lesser time span. The method presented in this paper showed promising results and could be used, for example, to monitor health of an individual, or the abuse of drugs, in infrared spectroscopy. It is possible that the use of these different types of proteins could be complementary to

each other to form a vast biological or medical monitoring system with photoacoustic infrared spectroscopy.

Acknowledgment The author would like to thank Dr. Tom Kuusela for supervising this study.

References

1. J.F. McClelland, R.W. Jones, S.J. Bajic, *Handbook of Vibrational Spectroscopy* (Wiley Ltd., Hoboken, NJ, 2006)
2. K.H. Michaelian, *Photoacoustic Infrared Spectroscopy* (Wiley Inc., New York, 2003)
3. A. Rosencwaig, Annu. Rev. Biophys. Bioeng. **9**, 31 (1980)
4. C.R. Robbins, *Chemical and Physical Behavior of Human Hair*, 4th edn. (Springer, New York, 2002)
5. D.J. Lyman, J. Murray-Wijelath, Appl. Spectrosc. **59**(1), 26 (2005)
6. K.S. Kalasinsky, Cell. Mol. Biol. **44**(1), 81 (1998)
7. K.S. Kalasinsky, J. Magluilo, T. Schaefer, Forensic Sci. Int. **63**, 253 (1993)
8. V. Signori, D.M. Lewis, Int. J. Cosmet. Sci. **19**, 1 (1997)
9. D.A. Scott, D.E. Renaud, S. Krishnasamy, P. Meric, N. Buduneli, S. Cetincalp, K.Z. Liu, Diabetol. Metab. Syndr. **2**(48), 1 (2010)
10. A. Sakudo, H. Kuratsune, Y.H. Kato, K. Ikuta, Clin. Chim. Acta **402**, 75 (2009)
11. S. Ekgasit, H. Ishida, Vib. Spectrosc. **19**, 1 (1996)
12. F. Fondeur, B.S. Mitchell, Spectrochim. Acta A **56**, 467 (2000)
13. N.A. Freebody, A.S. Vaughan, A.M. Macdonald, Anal. Bioanal. Chem. **396**, 2813 (2010)
14. T. Kuusela, J. Kauppinen, Appl. Spectrosc. Rev. **44**, 443 (2007)
15. V. Koskinen, J. Fonsen, K. Roth, J. Kauppinen, Appl. Phys. B **86**, 451 (2007)
16. R.E. Lindley, A.M. Parkes, K.A. Keen, E.D. McNaghten, A.J. Orr-Ewing, Appl. Phys. B **86**, 707 (2007)
17. R.G. Schipper, E. Silletti, M.H. Vingerhoeds, Arch. Oral Biol. **52**, 1114 (2007)
18. D.J. Lyman, P. Scofield, Appl. Spectrosc. **62**(5), 525 (2008)
19. L. Farren, S. Shayler, A.R. Ennos, J. Exp. Biol. **207**, 735 (2004)
20. M.G. Sowa, J. Wang, C.P. Schultz, M.K. Ahmed, H.H. Mantsch, Vib. Spectrosc. **10**, 49 (1995)
21. C.P. Schultz, M.K. Ahmed, C. Dawes, H.H. Mantsch, Anal. Biochem. **240**, 7 (1996)
22. R.O. Carter III, S.L. Wright, Appl. Spectrosc. **45**(7), 1101 (1991)
23. R.W. Jones, J.F. McClelland, Appl. Spectrosc. **55**(10), 1360 (2001)
24. J.L. Bantignies, G.L. Carr, D. Lutz, S. Marull, G.P. Williams, G. Fuchs, J. Cosmet. Sci. **51**, 73 (2000)
25. J. Strassburger, M.M. Breuer, J. Soc. Cosmet. Chem. **36**, 61 (1985)
26. P. Dumas, L. Miller, Vib. Spectrosc. **32**, 3 (2003)
27. L.E. Jurdana, K.P. Ghiggino, I.H. Leaver, C.G. Barraclough, P. Cole-Clarke, Appl. Spectrosc. **48**(1), 44 (1994)
28. S.Y. Venyaminov, N. Kalnin, Biopolymers **30**, 1243 (1990)